Acta of Bioengineering and Biomechanics
Vol. 15, No. 4, 2013

Original paper
DOI: 10.5277/abb130409

Stress distribution comparisons of foot bones in patient with tibia vara: a finite element study

ARIF ÖZKAN[1]*, HALIL ATMACA[2], İBRAHIM MUTLU[3], TALIP ÇELIK[3], LEVENT UĞUR[4], YASIN KIŞIOĞLU[3]

[1] Faculty of Engineering, Department of Biomedical Engineering, Duzce University, Konuralp Campus Duzce, Turkey.
[2] Department of Orthopaedics and Traumatology, Akdeniz University, Antalya, Turkey.
[3] Department of Mechanical Education, Technical Education Faculty Kocaeli University, Umuttepe Campus, Kocaeli, Turkey.
[4] Department of Automotive, Vocational High School Amasya University, Amasya, Turkey.

Blount's disease, or tibia vara, is the most common cause of pathologic genu varum in children and adolescents. Changes in the loading of knee structures such as tibial articular cartilage, menisci and subcondral bone are well documented in case of genu varum. But the mechanical effects of this condition on foot bones are still questionable. In this study, the authors hypothesized that stress distributions on foot bones might increase in patients with tibia vara when compared with patients who had normal lower extremity mechanical axis. Three-dimensional (3D) finite element analyses of human lower limb were used to investigate and compare the loading on foot bones in normal population and patient with tibia vara. The segmentation software, MIMICS was used to generate the 3D images of the bony structures of normal and varus malalignment lower extremity. Except the spaces between the adjacent surface of the phalanges fused, metatarsals, cuneiforms, cuboid, navicular, talus and calcaneus bones were independently developed to form foot and ankle complex. Also femur, tibia and fibula were modeled utilizing mechanical axis. ANSYS version 14 was used for mechanical tests and maximum equivalent stresses (MES) were examined. As a result of the loading conditions, in varus model MES on talus, calcaneus and cuboid were found higher than in normal model. And stress distributions changed through laterally on middle and fore foot in varus deformity model.

Key words: *tibia vara, genu varum, mechanical axis, load bearing*

1. Introduction

In terms of walking comfort and knee joint stabilization, mechanical axis should be located between femoral head globe and distal end of tibia at a vertical position passing through the center of knee joint. Varus deformity which is one of the tibia deformities affects the function of walking as it affects the load charged on cruciate ligaments. Blount's disease, or tibia vara, is the most common cause of pathologic genu varum in children and adolescents. Tibia vara has been classified as infantile, juvenile, and adolescent, the infantile form occurring before the age of 4, the juvenile form between 4 and 10 years of age and the adolescent form after 10 years [1].

Finite element analysis facilitates the efficient evaluation of different surgical techniques without the in-vivo surgery. Cheung et al. [2] calculated the stress values in foot bones through finite element method in their study. Bandak et al. [3] analyzed the stress in the ligament elements of the ankle through finite element method. Also some finite element studies in literature have shown the potentials in understanding lower extremity biomechanics [4], [5]. However, there is no study in the literature where comparison and evaluation of stress distribution on foot bones in normal model and varus malalignment model.

* Corresponding author: Arif Özkan, Faculty of Engineering, Department of Biomedical Engineering, Duzce University Konuralp Campus, 81340, Duzce, Turkey. Tel: +90542 235 9298, fax: +90380 542 1134, e-mail: arifozkan@duzce.edu.tr

Received: June 14th, 2012
Accepted for publication: June 10th, 2013

In this study, the authors hypothesized that stress distributions on foot bones might increase in patients with tibia vara when compared with patients who had normal lower extremity mechanical axis. Three-dimensional (3D) finite element analyses of human lower limb were used to investigate and compare the loading on foot bones in normal population and patient with tibia vara.

2. Materials and methods

2.1. Elements of lower extremity

The line starting from the center of femoral head globe and continuing up to the mid of ankle corresponds to the mechanical axis. Line passing through the shaft axis of such long bones as tibia and femur can be expressed as the mechanical axis of the bone to which it belongs. Relationship between proximal tibia, knee and mechanical axis in the frontal plan corresponds to the middle of knee joint or its 10 mm medial (inner part) when lower extremity mechanical axis is drawn. While outward angulation of the axis is defined as valgus deformity, it is called as varus deformity if the axis passes from inner part more than 17 mm (Fig. 1). Besides, varus deformity is expressed as angular deformation between the anatomical tibial axis and mechanical axis as shown in Fig. 1. In the present study, varus deformity was addressed.

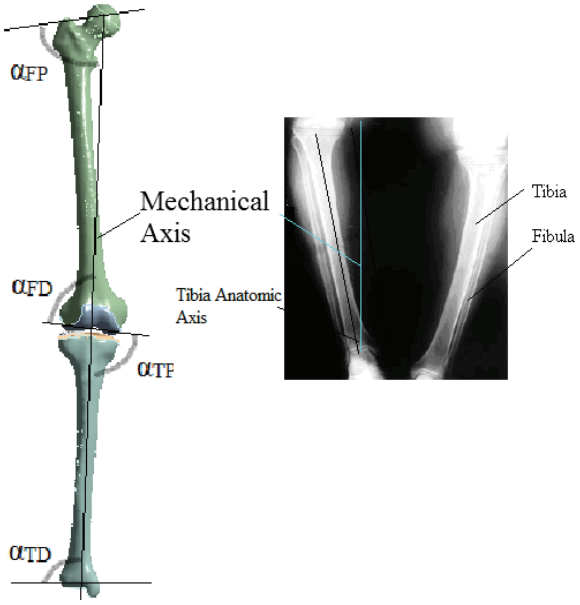

Fig. 1. Mechanical axis of lower extremity

Since lateral proximal femoral angle displayed as α_{FP} in Fig. 1 normally varies between 85° and 95°, its average value is accepted to be 90°. However, the average value for α_{TD} angle is 89° and values varying between 86° and 92° are deemed normal. In Fig. 2, ankle bones are displayed. As foot bones complete the load transfer under normal standing conditions, they are elements directly affected by the injury of lower extremity axis angles.

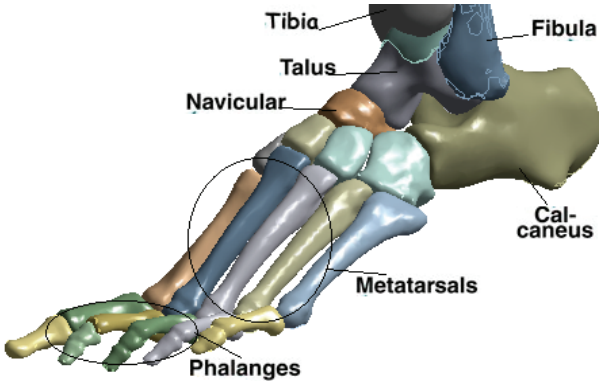

Fig. 2. Bones of foot and ankle joint

2.2. Three dimentional modelling of lower extremity structures

In the field of medicine, computer-aided planning before surgical operations to be conducted through such imaging techniques as Computed Tomography (CT) and Magnetic Resonance (MRI) are frequently used in recent years. In this study, main model was also modeled via CT images. CT images of the lower extremity bones for normal model were collected from our Institute folder archieve while varus model was obtained from a female patient aged 21 through Toshiba Aquilion CT scanner in the department of Radiology of the Faculty of Medicine in Kocaeli University. CT images consist of parallel layers having a section range of 0.774 mm at neutral position and a pixel resolution of 512 × 512. A 1841-layer shooting was carried out to develop the model used as reference. Images were recorded at dicom (Digital Imaging and Communications in Medicine) format. After these images were transferred into MIMICS 12.11 program which is a 3D image processing software, 3D model displayed in Fig. 3 was obtained.

All bone structure models and geometric arrangements were completed through reverse engineering program (GEOMAGIC®). After the correction of surface errors of deformative and corrected models, 3D smooth solid models were developed.

Once the geometric arrangements of the models had been completed, finite elements models were obtained by transferring them into MIMICS® FEA (finite element analysis module) content in STL (Steriolithography) format.

Varus deformity

Fig. 3. 3D models of lower extremity and ankle bones

2.3. Calculation of load distribution

To compare the load distributions observed in bones of ankle joint and foot, finite elements models of deformative and normal lower extremities were transferred into ANSYS® WORKBENCH software through MIMICS® FEA interface. 10 node tetrahedral elements were used for mesh of finite element models. Computer-aided finite element analysis aimed at comparing the load distributions was carried out through ANSYS® WORKBENCH software.

2.3.1. Material properties of bone and non-bone structures

In this study, it was assumed that bone structures in the developed models were elastic and isotropic. Furthermore, visicoelastic material properties of the bone structure were identified. Identification of visicoelastic properties of the bone structure in ANSYS® WORKBENCH material editor was carried out by entering bulk module 2.3 GPa [6], [7] and shear module [6]–[8]. Material properties of bone, cartilage and meniscus were identified at values given in Table 1.

Table 1. Material properties of bones and non-bone structures [6]–[12]

Structure	Modulus of elasticity (E) MPa	Poisson's ratio (v)
Femur	17.000	0.3
Tibia	14.000	0.3
Calcaneus and other foot bones	5.000	0.3
Menisci	59	0.49
Cartilage	5	0.46

2.3.2. Boundary and loading conditions

Load put on foot bones varies by the movement of human and the position of standing. The fact that load put on by human body is transferred through hip and knee joints was taken into consideration to calculate load carrying capacities of elements constituting the lower extremity. In the study conducted by Simoes et al. [11] on different loads such as muscle loads affecting the body weight and proximal femur, body

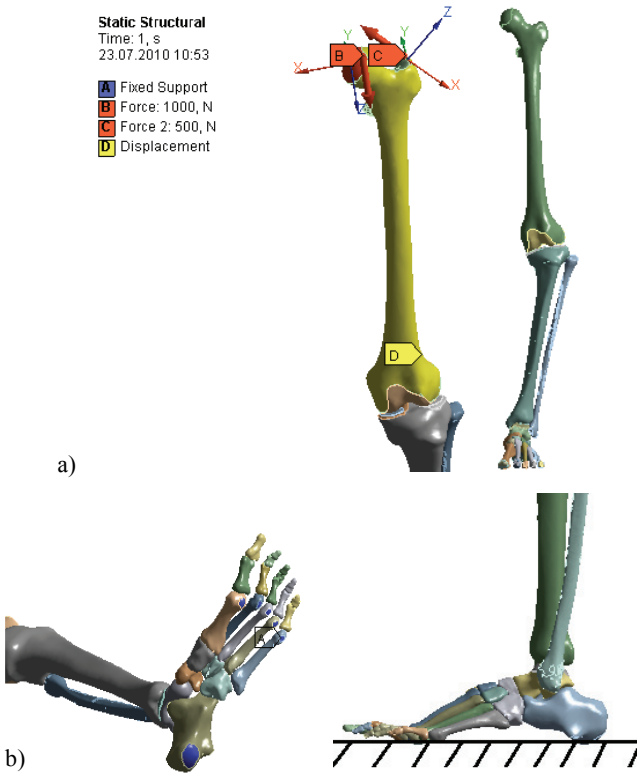

Fig. 4. FEA loading conditions of lower extremity

burden was identified as 700 N and the abductor force was identified as 300 N. On the other hand, in the study carried out by Moreo et al. [12], body burden was used as 2092 N and the abductor force was used as 975 N. Considering all these data, body weight of 1000 N displayed in Fig. 4 was applied to the surface of femoral head globe in contact with hip joint. As a component of the muscle loads, abductor load was put on toward pelvis through the trochanter major of femur as 500 N.

Due to normal movement axis of muscle and ligament, a degree of freedom was identified to the femoral bone only in line with mechanical axis. Surfaces of calcaneus and the other foot bones in contact with ground were completely stabilized as shown in Fig. 4b (zero displacement). Same loading and boundary conditions were determined in both models. A 10 node tetra element was used for the finite element models obtained under the aforementioned material properties and loading and boundary conditions and models contained 242.235 elements on average. Except the spaces between the adjacent surfaces of the phalanges fused, metatarsals, cuneiforms, cuboid, navicular, talus and calcaneus bones were independently developed to form foot and ankle complex.

Table 2. FEA results of structures in normal and varus deformity models (MPa)

Structure	MES in normal model (MPa)	MES in varus model (MPa)
Talus	31.8	56.9
Calcaneus	36.7	55.4
Navicula	20.1	18.9
Cuboid	10.8	18.3
Medial cuneiform	5.9	6.7
Middle cuneiform	8.8	11.7
Lateral cuneiform	4.1	4.8
1st metatarsal	7.1	4.9
2nd metatarsal	6.7	6.3
3rd metatarsal	6.8	7.8
4th metatarsal	2.3	6.9
5th metatarsal	2.1	4.6
1st toe	3.2	2.8
2nd toe	1.6	1.5
3rd toe	0.5	0.4
4th toe	0.6	0.6
5th toe	0.7	0.9

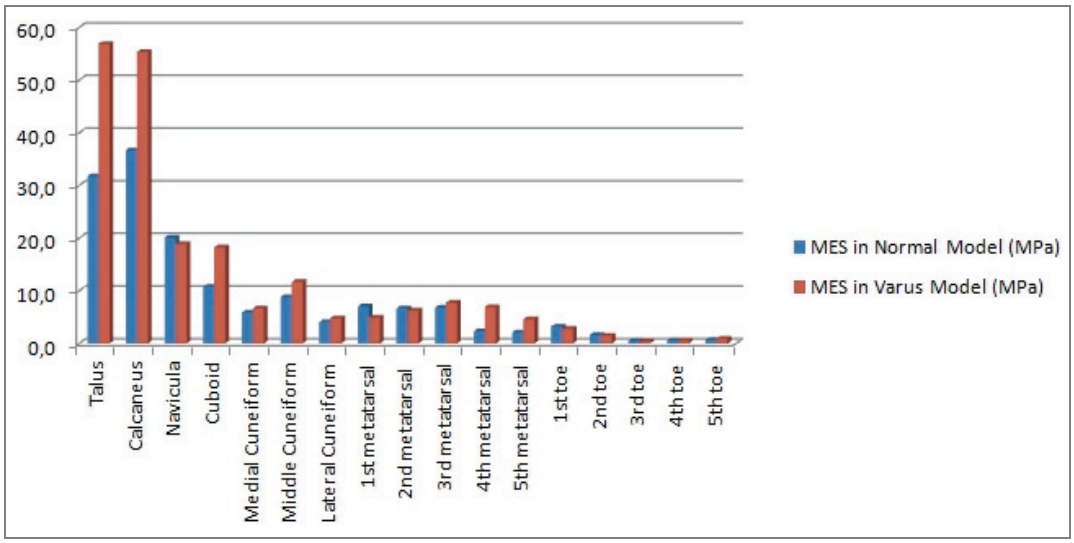

Fig. 5. Comparable load distribution on foot bones at same structure of varus deformity normal models (MPa)

3. Results

In terms of stress distribution in ankle complex and rear foot; MES were higher on all bones except navicula in varus model when compared with normal one. The results of MES are given in Table 2. On the other hand, load bearing was increased through laterally in varus model on bones at mid and front foot (Table 2). Comparable graphics of results among same structures are given in Fig. 5.

4. Discussion

The analysis results showed that the stresses in rear foot of the varus foot-ankle increased to a normal foot-ankle. Whereas, the equivalent stresses of navic-

ula, first and second metatarsals were decreased. So, these results showed correlation by supporting the authors' hypothesis which claims increased loading on foot bones additionally to knee structures in patient with tibia vara.

Pain and knee arthrosis are the natural long-term result of untreated cases of Blount's disease by increased adduction moment due to varus mechanical axis [13]. Although a metaphyseal osteotomy with acute correction and internal or external fixation is the state of the art treatment of infantile tibia vara, this has been found to be less appropriate in treating late-onset tibia vara [1]. Kurosawa and Doi [14] demonstrated that tibia vara is a primary determinant of joint compression forces at the knee. They took radiographic measurements of tibia vara and the femorotibial angle and found that a higher correlation existed between tibia vara and knee joint compression forces. In a study based on a finite element model study, Cook et al. [15] concluded that increasing varus resulted in increasing compressive stress in the medial tibial physis, up to a level of seven times more than the normal level when the varus was in a position at 30°. Further, tensile stresses determined in the lateral tibial physis were increased above normal. The main superiority of the current study to previous studies was to investigate stress distribution on foot bones in patient with tibia vara. Stress distribution (MPa) on the talus in a case of tibia vara: (A) lateral view; (B) plantar view. MES on the talus was obtained in the subtalar articular surface. Thus, patients with varus malalignment may be candidates for subtalar arthritis (Fig. 6).

In critically analyzing the data, applied loads were distributed through laterally especially at middle and front foot in model with tibia vara (Fig. 5). This may be as a result of modified longitudinal and medial arc of foot to accommodate the deformed mechanical axis due to varus deformity. The relationship between tibia vara and calcaneal eversion is especially important for the function of the lower extremity. The degree of calcaneal eversion present in standing and walking must at least be equal to the degree of tibia vara, so that the foot can prorate to allow the calcaneus to rest flat on the supporting surface [14], [15].

Varus deformity can usually be corrected through proximal tibial open or closed osteotomies (PTO). The aim of PTO surgery is to transfer the stress to the healthy lateral (external) meniscus compartment. This surgery eliminates the deformity by correcting the varus deformity and positioning the tibia toward the mechanical axis [16]–[18]. This study showed increased stresses on foot bones in case of tibia vara. Although the current study mainly suffers from only evaluating foot bones bearing by ignoring knee structures such as menisci and cartilage, it may lead future studies that investigate the effect of tibial corrective osteomies on menisci, cartilage and foot bones.

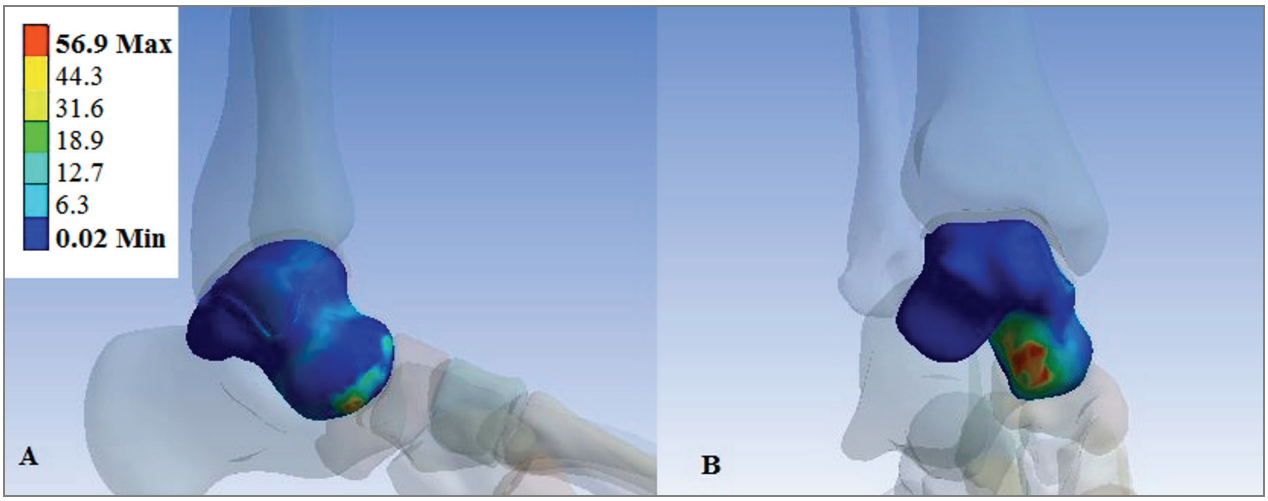

Fig. 6. Stress distribution (MPa) on the talus in the case of tibia vara:
(A) lateral view; (B) plantar view. MES on the talus was obtained in the subtalar articular surface.

References

[1] AMER A.R., KHANFOUR A.A., *Evaluation of treatment of late-onset tibia vara using gradual angulation translation high tibial osteotomy*, Acta Orthop. Belg., 2010, Vol. 76(3), 360–366.

[2] CHEUNG J.T., ZHANG M., *A 3D finite element model of the human foot and ankle for insole design*, Arch. Phys. Med. Rehabil., 2005, Vol. 86, 353–358.

[3] BANDAK F.A, TANNOUS R.E., TORIDIS T., *On the development of an osseo-ligamentous finite element model of the human ankle joint*, Int. J. Solids Struct., 2001, Vol. 38(10–13), 1681–1697.

[4] BARANI Z., HAGHPANAHI M., KATOOZIAN H., *Three-dimensional stress analysis of diabetic insole: a finite element approach*, Technol. Health Care, 2005, Vol. 13, 185–192.

[5] CHEN W.P., JU C.W., TANG F.T., *Effects of total contact insoles on the plantar stress redistribution: a finite element analysis*, Clin. Biomech., 2003, Vol. 18, S17–24.

[6] ASHMAN R.B., COWIN S.C., VAN BUSKIRK W.C., RICE J.C., *A continuous wave technique for the measurement of the elastic properties of cortical bone*, J. Biomech., 1984, Vol. 17, 349–361.

[7] REILLY D.T., BURSTEIN A.H., *The mechanical properties of cortical bone*, J. Bone Joint Surg., 1974, Vol. 56A, 1001, 1022.

[8] MARTENS M., VAN AUDEKERCKE R., DEMEESTER P., MULIER J.C., *The geometrical properties of human femur and tibia and their importance for the mechanical behaviour of these bone structures*, Arch. Orthop. Trauma Sur., 1981, Vol. 98, 113–120.

[9] MARTENS R., VAN AUDEKERCKE R., DELPORT P., DEMEESTER P., MULIER J.C., *The mechanical characteristics of cancellous bone at the upper femoral region*, J. Biomech., 1983, Vol. 16, 971–983.

[10] YAMADA H., *Mechanical Properties of Locomotor Organs And Tissues, Strength of Biological Materials*, Williams & Wilkins, Baltimore, 210 p., 1970.

[11] SIMOES J.A., VAZ M.A., BLATCHER S., TAYLOR M., *Influence of head constrains and muscle forces on the strain distribution within the intact femur*, Med. Eng. Phys., 2000, Vol. 22, 453–459.

[12] MOREO P., PÉREZ M.A., GARCÍA-AZNAR J.M., *Modelling the mechanical behaviour of living bony interface*, Comp. Methods Appl. Mech. Engr., 2007, Vol. 196, 3300–3314.

[13] CHOTIGAVANICHAYA C., SALINAS G., GREEN T., MOSELEY C.F., OTSUKA N.Y., *Recurrence of varus deformity after proximal tibial osteotomy in Blount disease: long-term follow-up*, J. Pediatr. Orthop., 2002, Vol. 22, 638–641.

[14] KUROSAWA H., Doi T., *Joint force analysis in degenerative varus or valgus knees during standing: importance of tibial tilt to the floor*, Nippon Seikeigeka Gakkai Zasshi, 1981, Vol. 55, 509–518.

[15] COOK S.D., LAVERNIA C.J., BURKE S.W., *A biomechanical analysis of the etiology of tibia vara*, J. Pediatr. Orthop., 1983, Vol. 3(4), 449–454.

[16] VAN HUYSSTEEN A.L., HASTINGS C.J., OLESAK M., HOFFMAN E.B., *Double-elevating osteotomy for late-presenting infantile Blount's disease: the importance of concomitant lateral epiphysiodesis*, J. Bone Joint Surg. Br., 2005, Vol. 87, 710–715.

[17] AOKI Y., YASUDA K., MIKAMI S., OHMOTO H., MAJIMA T., MINAMI A., *Inverted V-shaped high tibial osteotomy compared with closing wedge high tibial osteotomy for osteoarthritis of the knee: 10 year follow-up result*, J. Bone Joint Surg. Br., 2006, Vol. 88, 1336–1340.

[18] RAB G.T., *Oblique tibial osteotomy for Blount's disease (tibia vara)*, J. Pediatr. Orthop., 1988, Vol. 8, 715–720.